

PAPER • OPEN ACCESS

## Fabrication and characterization of 1, 5, 10 at.% Ce:Y<sub>2</sub>O<sub>3</sub> nanopowders

To cite this article: K E Lukyashin *et al* 2020 *IOP Conf. Ser.: Mater. Sci. Eng.* **848** 012051

View the [article online](#) for updates and enhancements.



The banner features a background image of Earth from space. On the left, there are three circular logos: the ECS logo, the Electrochemical Society logo, and The Korean Electrochemical Society logo. The central text reads: "The best technical content in electrochemistry and solid state science and technology!" Below this, a blue bar contains the text "Available until November 9, 2020." On the right, the PRIME 2020 logo is displayed, with the text "PACIFIC RIM MEETING ON ELECTROCHEMICAL AND SOLID STATE SCIENCE" and "2020". At the bottom right, a dark blue box contains the text "REGISTER TO ACCESS CONTENT FOR FREE!" with a right-pointing arrow.

**ECS**

**The best technical content in electrochemistry and solid state science and technology!**

**Available until November 9, 2020.**

**PRIME<sup>TM</sup>**  
PACIFIC RIM MEETING  
ON ELECTROCHEMICAL  
AND SOLID STATE SCIENCE  
**2020**

**REGISTER TO ACCESS  
CONTENT FOR FREE! ▶**

# Fabrication and characterization of 1, 5, 10 at.% Ce:Y<sub>2</sub>O<sub>3</sub> nanopowders

K E Lukyashin<sup>1</sup>, A S Chepusov<sup>1</sup> and V I Solomonov<sup>1,2</sup>

<sup>1</sup> Institute of Electrophysics UrB RAS, Yekaterinburg, Russia

<sup>2</sup> Ural Federal University, Yekaterinburg, Russia

E-mail: [kostya@iep.uran.ru](mailto:kostya@iep.uran.ru)

**Abstract.** Nanopowders (particle size of about 7-14 nm) of yttrium oxide doped with cerium ions with concentrations of 1, 5, 10 at.% have been synthesized by laser ablation of the target. For the first time in the world the cerium concentration of 10 at.% in the yttrium oxide lattice has been obtained. Their morphology, structure, and scintillation properties have been investigated. No significant cathodoluminescence of the activator in the Ce<sup>3+</sup> state has been detected in the powders, and X-ray luminescence was completely absent. Presumably, the cerium ion is in the nonradiative state of Ce<sup>4+</sup>.

## 1. Introduction

Ceramic materials research continues to evolve around the world. Moreover, one of the main advantages of ceramics is the possibility of doping a large number of active centers [1] with concentrations up to 30 at.% [2], which is not achievable in single crystals, where the threshold does not exceed 1 at.%.

One of the applications of ceramics is their use as scintillators. Yttrium aluminum garnet doped with cerium ions is a well-known and well-established scintillation material. Previously, this material was already synthesized and examined by the authors. So, for example, we have already demonstrated the relative light yield surpassing its analogues for single crystals and making up 32% of one of the CsI-Tl reference scintillator (light output 20800 photon/MeV) at the cerium concentration of 1 at.%, in our paper on the synthesis and characterization of the optical-luminescent properties of Ce<sup>3+</sup>:YAG ceramics with different Ce concentrations (0.1 - 5 at.%) [3]. In addition, an increase in the speed of the scintillator was recorded (from 110 to 26 ns) with an increase in the concentration of cerium activating ions (from 0.1 to 5 at.%). It can be assumed that a further increase in the concentration of cerium ions, for example, up to 10 at.%, will lead to even greater speed. The authors believe that this is possible, and this is due to the concentration quenching effect.

Due to its unique scintillation properties, Ce:YAG is used as an X-ray and soft gamma-ray detector [4, 5]; it is characterized by high efficiency, mechanical and thermal stability. At the same time, there is a problem of correct registration of short (ns) X-ray radiation pulses and measurements of dose loads [6], which (pulsed radiation) are increasingly used in science and technology as more effective (Decreasing the dose load on people or inanimate objects by tens of times, reducing by times the mass and size parameters of X-ray sources). It is planned to solve this problem by synthesizing a new ceramic material based on yttrium aluminum garnet.

At the first stage of research, it is necessary to obtain and characterize nanopowders of the corresponding composition, which are needed in the synthesis of Ce:YAG ceramics. For a



comprehensive study and construction of the corresponding physical and mathematical model in the future, three compositions of 1, 5, 10 at.% Ce:Y<sub>2</sub>O<sub>3</sub> nanopowders were chosen.

Thus, the aim of this work is to synthesize and characterize Y<sub>2</sub>O<sub>3</sub> nanopowders doped with cerium ions with 1, 5, 10 at.% contents of the latter for the synthesis of new high-speed ceramic Ce:YAG scintillators for detecting nanosecond X-ray radiation pulses.

## 2. Experimental

Yttrium oxide nanopowders doped with cerium ions with concentrations of 1, 5, 10 at.% were synthesized by laser ablation of a solid porous target [7]. The cerium concentration of 10 at.% in the yttrium oxide lattice was obtained for the first time in the world. This method makes it possible to distribute the dopant evenly in the main material still at the synthesis stage, whereby it is immediately incorporated into the lattice of the main material. In this case, cerium ions replace yttrium ions.

The synthesized nanopowders were studied using a JEOL JEM 2100 (JEOL Ltd., Japan) transmission electron microscope (TEM). The specific surface area of powders (BET analysis) was determined by an automated gas adsorption analyzer (TriStar 3000, Micromeritics Instrument Corporation, USA). The structures of the sintered nanopowders were determined by X-ray diffraction (XRD) on copper radiation (CuK $\alpha$ ,  $\lambda = 1.542\text{\AA}$ ) with the graphite monochromator on a secondary beam (D8 Discover GADDS, Bruker AXS, Germany). The processing of the XRD results was carried out via the full-height analysis program named TOPAS 3.

The pulsed cathodoluminescence (PCL) and X-ray luminescence (XRL) of powders were measured both immediately after their laser synthesis and after their transformation in the main cubic phase at 900°C for 3 hours in an atmospheric furnace. In addition, compacts fabricated from the obtained nanopowders by pressing at 200 MPa into disks ( $\varnothing 14 \times 3$  mm) were examined.

The luminescent properties in the range 220–850 nm were measured by pulsed cathodoluminescent spectroscopy method (PCL) using our own KLAIVI setup (IEP, Russia) with the maximum electron energy in the beam of 180 keV, pulse duration of 2 ns, pulse repetition rate of 1 Hz, and electron current density of 120 A/cm<sup>2</sup> [8]. The PCL spectrum was recorded in air at room temperature of the samples using a multichannel photodetector based on a CCD array combined with a diffraction spectrograph. The pulse X-ray luminescence (XRL) spectra were measured using an experimental generator of nanosecond X-ray radiation pulses consisting of two main parts: a high-voltage generator and a pulsed explosive-emission tube (IEP, Russia). The signal was measured using an experimental setup based on MicroFC 60035 photodiodes and a Tektronix TDS648 oscilloscope. Unique output characteristics of the used high-voltage generator (voltage amplitude up to 115 kV, pulse duration at half maximum up to 50 ns) require a special X-ray tube for operation as a source of pulsed X-ray radiation. The axially-symmetrical explosive-emission tube and a blade metal cathode were used in this case. The measurements were carried out with the X-ray radiation exposure of 1 s at the pulse repetition rate of 2 kHz.

## 3. The Results and Discussion

The morphological properties of the synthesized nanopowders were examined by scanning electron microscopy methods. For example, Figure 1 shows an image of the synthesized 1 at.% Ce:Y<sub>2</sub>O<sub>3</sub> nanopowder and the size distribution function of nanoparticles taken after counting 4000 particles. It can be seen that the particles have an almost perfect spherical shape (Figure 1a). From the particle size distribution (Figure 1b), we observe that the peak falls at 11 nm, and the average particle size is 7-14 nm. The distribution lies in a very narrow range. Similar data were obtained for the other two powder compositions.

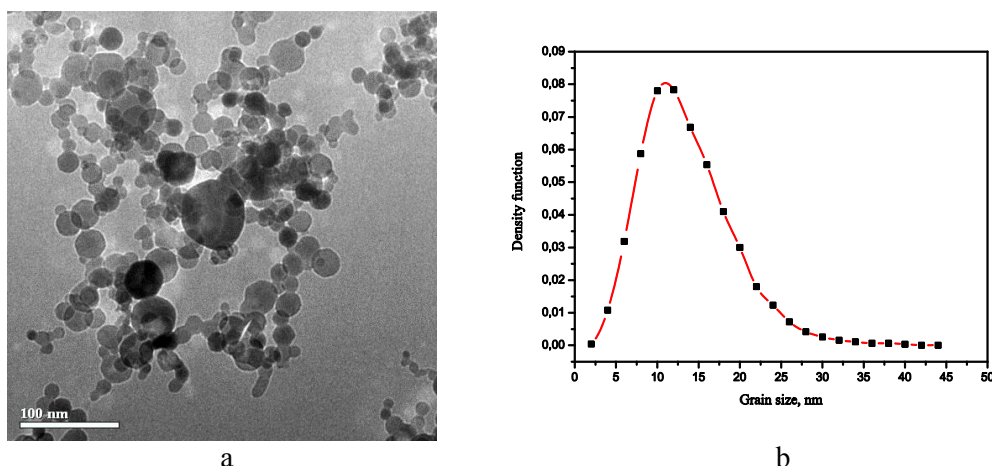


**Figure 1.** Transmission electron microscopy (TEM) images of 1 at.%Ce:Y<sub>2</sub>O<sub>3</sub> nanopowders produced by the laser ablation method (a). Size distribution of the nanopowders (b).

The structure of the powders was confirmed using X-ray diffraction analysis (XRD), the results of which are presented in Table 1. All powders have been obtained in a metastable monoclinic phase. The powder with the cerium content of 10 at.% stands out against the overall picture; it has been found that it contains a second phase (cubic cerium oxide CeO<sub>2</sub>) with the content of about 3 wt.%. The presence of the second phase indicates that the cerium oxide has been unable to be incorporated into the lattice of the yttrium oxide in full, but has remained in the initial state partly. In addition, it is worth noting that, according to the same XRD results, the coherent scattering region (CSR) of particles decreases with the cerium concentration increase.

**Table 1.** XRD results.

Sample	mon – Y <sub>2</sub> O <sub>3</sub> (main phase)				
	SCR, nm	Lattice constants, Å			
1 at.%Ce:Y <sub>2</sub> O <sub>3</sub>	24±2	a = 13.921±0.007	b = 3.496±0.002	c = 8.614±0.005	β=100.19°
5 at.%Ce:Y <sub>2</sub> O <sub>3</sub>	22±2	a = 13.91±0.02	b = 3.502±0.005	c = 8.62±0.02	β=100.28°
10 at.%Ce:Y <sub>2</sub> O <sub>3</sub> *	20±3	a = 13.910±0.008	b = 3.510±0.002	c = 8.639±0.005	β=100.41°

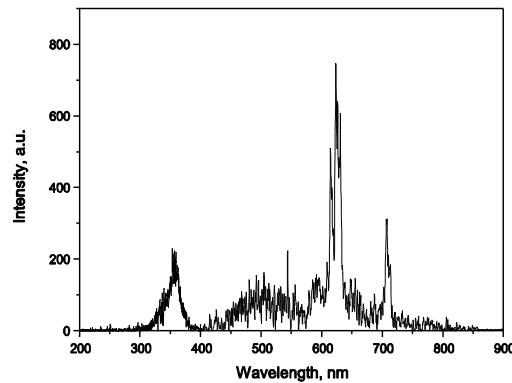
\* The sample with 10 at.% of Ce:Y<sub>2</sub>O<sub>3</sub> contains the second phase: CeO<sub>2</sub> (Cerianite, cubic, content ≈3 wt.%), SCR = 29±3 nm, a = 5.327±0.005 Å

The results of the analysis of the specific surface area of particles (BET) show (Table 2) that the specific surface area increases with the increase in the concentration of the cerium activating ion, that is, the particle size decreases. This is also evidenced by the SCR data given in Table 1. This fact indicates that, when being incorporated into, cerium inhibits the growth of nanoparticles and distorts the yttrium oxide lattice, because their ionic radii are different: Y<sup>3+</sup> (0.122 nm), Ce<sup>4+</sup> (0.128 nm), Ce<sup>3+</sup> (0.148 nm).

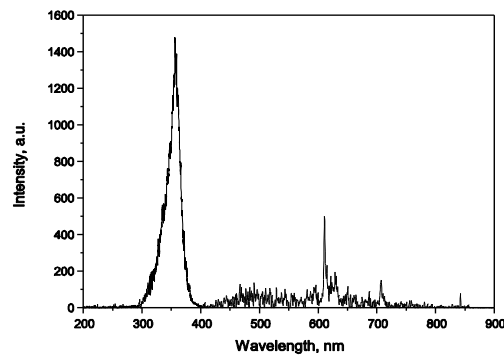
**Table 2.** Characteristics of synthesized nanoparticles.

	1 at.% Ce:Y <sub>2</sub> O <sub>3</sub>	5 at.% Ce:Y <sub>2</sub> O <sub>3</sub>	10 at.% Ce:Y <sub>2</sub> O <sub>3</sub>
Specific surface area (BET analysis), m <sup>2</sup> /g	50.5152	51.01128	52.7950
Diameter of particles calculated upon BET data, nm	21.83	21.62	20.89
SCR (XRD), nm	24±2	22±2	20±3

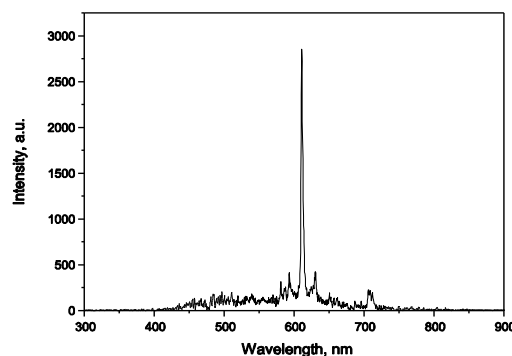
Studies have shown that the PCL spectra of the powders and compacts are qualitatively similar to each other (Figure 2).



a



b



c

**Figure 2.** PCL spectra of compacts: monoclinic phase 1 at.% Ce:Y<sub>2</sub>O<sub>3</sub> (a), cubic phase 1 at.% Ce:Y<sub>2</sub>O<sub>3</sub> (b), cubic phase 10 at.% Ce:Y<sub>2</sub>O<sub>3</sub> (c).

In the spectral range 400–850 nm, the luminescence of the intrinsic surface center (bound radical Y-O) in the form of a system of narrow bands and a broad band with a center of about 500 nm has been observed in all spectra [8–10]. The band with a maximum at 350 nm, shown in Figure 2a,b, is emitted by self-trapped excitons (STEs), which are O<sup>2-</sup> hole centers associated with the Y<sup>3+</sup> vacancy [10]. The luminescence of these STEs has been observed only in the nanopowders with the cerium content of 1 at.%. Moreover, in the nanopowders of the cubic phase (Figure 2b), their luminescence

intensity increases by almost an order of magnitude, compared with the monoclinic phase (Figure 2a). However, with an increase in the cerium content, this band disappears from the PCL spectrum (Figure 2c), i.e. cerium helps to eliminate this defect. However, the luminescence bands of  $\text{Ce}^{3+}$  ions are absent in the PCL spectra of the nanopowders with different cerium contents. This situation may be due to the fact that cerium in the  $\text{Ce:Y}_2\text{O}_3$  nanopowders is in the tetravalent state  $\text{Ce}^{4+}$ , which is inactive in luminescence.

Pulsed X-ray luminescence (XRL) of the powders and compacts of the monoclinic and cubic phases was not detected. It should be noted that the XRL is much weaker than the PCL, due to the smaller cross section for radiation-matter interaction.

#### 4. Conclusions

The method of laser ablation of a solid porous target was used to synthesize  $\text{Y}_2\text{O}_3$  nanopowders doped with cerium ions with the content of the latter 1, 5, 10 at.%. The yttrium oxide nanopowder with the cerium (Ce) activating ion content of 10 at.% has been obtained for the first time in the world. The obtained nanopowders are in a metastable monoclinic phase, have an almost perfect spherical shape and an average particle size of 7-14 nm. The second phase was detected in the powder with 10 at.% of  $\text{Ce:Y}_2\text{O}_3$ : the undissolved cerium oxide  $\text{CeO}_2$  in a cubic modification with a content of  $\approx 3$  wt.%. In all powders, the pulsed X-ray luminescence has not been excited, but the pulsed cathodoluminescence has been well excited. Its spectra for free and compacted powders have been similar. The intrinsic center luminescence bands of Y-O and STE type dominate in them, but no luminescence bands of the  $\text{Ce}^{3+}$  ions have been detected. Apparently, the cerium ion in  $\text{Ce:Y}_2\text{O}_3$  nanopowders is in the tetravalent state, which is inactive in luminescence. Nevertheless, the obtained nanopowders can be used for the synthesis of new high-speed ceramic Ce:YAG scintillators for detecting nanosecond X-ray radiation pulses.

#### Acknowledgments

The reported study was funded by RFBR, project number 19-08-00117.

The authors gratefully acknowledge E.V. Tihonov and Dr. A.I. Medvedev from Institute of Electrophysics UrB RAS for laser synthesis of nanopowders and XRD analysis, respectively.

#### References

- [1] Tokurakawa M., Takaichi K., Shirakawa A. et al 2007 *Appl.Phys.Lett.* **90** (5) 071101\_1-071101\_3
- [2] Mourona J., Dujardin C., Tillement O. et al 2008 *J. Alloys and Comp.* **464** 407-411
- [3] Osipov V., Ishchenko A., Shitov V. et al 2017 *Opt.Mat.* **71** 98-102
- [4] Kobayoshi M., Shinkawa T., Sato T. et al 1994 *Nucl.Instr.Meth.* **A337** 355
- [5] Fyodorov A., Pavlenco V., Korzhik M. et al 1996 *Radiat.Meas.* **26** (2) 215
- [6] Miloichikova I. et al 2014 *IOP Conf.Ser.: Mat.Sci. and Eng.* **66** (012031) 4
- [7] Osipov V., Kotov Yu. et al 2006 *Las. Phys.* **16** 116-125
- [8] Osipov V., Solomonov V., Spirina A. 2011 *J.Opt.Technol.* **78** 408-412
- [9] Osipov V., Rasuleva A., Solomonov V. 2008 *J.Opt. Spectrosc.(Russia)* **105** (4) 591-597
- [10] Solomonov V., Osipov V., Shitov V., Lukyashin K., Bubnova A. 2020 *J. Opt. Spectrosc.(Russia)* **128** (1) 5-9